Smart Structures and Systems, *Vol. 29, No. 4 (2022) 641-652*
https://doi.org/10.12989/sss.2022.29.4.641

Compound damping cable system for vibration control of high-rise structures

Jianda Yu [1,3a], Zhouquan Feng[*2,4,5], Xiangqi Zhang [1b], Hongxin Sun [1,3c] and Jian Peng [1,3d]

[1] *School of Civil Engineering, Hunan University of Science and Technology, Xiangtan 411201, China*
[2] *College of Civil Engineering, Hunan University, Changsha 410082, China*
[3] *Hunan Provincial Key Laboratory of Structures for Wind Resistance and Vibration Control, Hunan University of Science and Technology, Xiangtan 411201, China*
[4] *Key Laboratory of Wind and Bridge Engineering of Hunan Province, College of Civil Engineering, Hunan University, Changsha 410082, China*
[5] *State Key Laboratory of Advanced Design and Manufacturing for Vehicle Body, Hunan University, Changsha 410082, China*

(*Received January 17, 2020, Revised October 20, 2021, Accepted October 23, 2021*)

Abstract. High-rise structures prone to large vibrations under the action of strong winds, resulting in fatigue damage of the structural components and the foundation. A novel compound damping cable system (CDCS) is proposed to suppress the excessive vibrations. CDCS uses tailored double cable system with increased tensile stiffness as the connecting device, and makes use of the relative motion between the high-rise structure and the ground to drive the damper to move back-and-forth, dissipating the vibration mechanical energy of the high-rise structure so as to decaying the excessive vibration. Firstly, a third-order differential equation for the free vibration of high-rise structure with CDCS is established, and its closed form solution is obtained by the root formulas of cubic equation (Shengjin's formulas). Secondly, the analytical solution is validated by a laboratory model experiment. Thirdly, parametric analysis is conducted to investigate how the parameters affect the vibration control performance. Finally, the dynamic responses of the high-rise structure with CDCS under harmonic and stochastic excitations are calculated and its vibration mitigation performance is further evaluated. The results show that the CDCS can provide a large equivalent additional damping ratio for the vibrating structures, thus suppressing the excessive vibration effectively. It is anticipated that the CDCS can be used as a good alternative energy dissipation system for vibration control of high-rise structures.

Keywords: compound damping cable system; equivalent additional damping ratio; high-rise structure; parametric analysis; vibration control

1. Introduction

With the growth of economy and the progress of technology, a variety of high-rise structures (such as skyscraper, wind turbine, power transmission tower, bridge tower, industrial chimney, television tower, etc.) have been constructed or under construction. These high-rise structures are slender and flexible with small damping, which are prone to large vibrations under the action of strong winds and lead to fatigue damage even collapse (Roy *et al*. 2012), causing grave loss of life and property, as a result, the vibration control of high-rise structures has been widely concerned (Li *et al*. 2011, Lu *et al*. 2017, Sun *et al*. 2019a, Zhang *et al*. 2013, Zuo *et al*. 2017).

The vibration reduction measures for high-rise structures mainly include dynamic vibration absorbers and energy dissipation devices. Examples of the former include tuned mass dampers (TMDs) (Lin *et al*. 2017, Lu *et al*. 2017, Sun *et al*. 2019a, Zahrai and Froozanfar 2019), tuned liquid column dampers (TLCDs) (Zhang *et al*. 2015, 2016), tuned inerter dampers (Lazar *et al*. 2014, Shen *et al*. 2019, Sun *et al*. 2019b), and some other inerter systems (Huang *et al*. 2019, Ikago *et al*. 2012a, b, Pan *et al*. 2018, Pan and Zhang 2018, Wang *et al*. 2019a, b, Zhang *et al*. 2019b), etc. Examples of the latter include fluid viscous dampers (FVD) (Lin and Chopra 2002), hysteretic dampers (Benavent-Climent 2011, Suarez *et al*. 2017), magnetorheological (MR) dampers (Aly *et al*. 2011, Duan *et al*. 2019, Zhang *et al*. 2019a) and eddy current dampers (Liang *et al*. 2019, Niu *et al*. 2018, Zuo *et al*. 2011), etc. Many famous high-rise structures such as Taipei 101, Canton Tower and Shanghai Tower all adopt TMD for wind induced vibration control. Zhang *et al*. (2013) adopted pounding TMD to control the first-order vibration mode of transmission towers. Tuned mass dampers in vibration suppression of structures with a single mode has a good performance, but it works poor if multiple vibration modes exist. A variety of new high-rise structures appear in recent years, and the fundamental frequencies of these structures are low and vibration with multiple modes may occur (Mao *et al*. 2018). The existing TMD technology can only slightly increase the equivalent additional damping ratio of the structure, which is difficult

*Corresponding author, Ph.D., Associate Professor,
E-mail: zqfeng@hnu.edu
[a] Professor
[b] Graduate Student
[c] Professor
[d] Associate Professor

ISSN: 1738-1584 (Print), 1738-1991 (Online)

to meet the demand of low fundamental frequency and multi-mode vibration reduction of high-rise structures such as wind turbine tower with increasing height.

Energy dissipation dampers have been successfully applied to control of cable vibration in several cable-stayed bridges (Chen *et al*. 2004, Gao *et al*. 2021, Li *et al*. 2007, Shi *et al*. 2016). The relative motion between the cable and the bridge deck is used to drive the damper to dissipate the cable vibration energy and suppress the multi-mode vibration of the cable. Since dampers require relative motion between the vibration structure and the surrounding objects to drive them to dissipate energy, it's not convenient to applied dampers to control the high-rise structures. One approach for control vibration of high-rise buildings is diagonal bracing in series with dampers to control the inter-story drifts (Ikago *et al*. 2012a, b, Liu *et al*. 2019, Wen *et al*. 2017). Another way to suppress the large vibration of high-rise structures is to utilize stabilizing cables. The cable directly connects the structure with the ground, which increase the stiffness of the structure and reduce the vibration amplitude of the structure. Due to the convenience of stabilizing cable construction, wind resistance by stabilizing cables for actual engineering structures has been widely applied (Choi and Kim 2008, Kim *et al*. 2013, Ni *et al*. 2005). However, if the length of the cable is too long, the sag effect will reduce the tensile stiffness of the cable and degrade the control performance of the stabilizing cables. On the other hand, damped cable system has also been proposed for seismic protection of structures (Sorace and Terenzi 2012a, b), where prestressed steel cables linked to pressurized fluid viscous spring-dampers is fixed to the foundation at their lower ends, and to the top floor, or one of the upper floors, at their upper ends. The cables have sliding contacts with the floor slabs, to which they are joined by steel deviators, and in this way a long cable is divided into multiple segments of short cables to reduce the sag effect. It belongs to the inter-story drift protective technologies, which is effective for multiple-story building structures but may not be applicable for other high-rise structures without distinct inter-story drift such as wind turbines, bridge towers, transmission tower and industrial chimney.

In view of the demand of multi-mode and ultra-low frequency vibration reduction of existing high-rise structures, Yu *et al*. (2014) proposed a compound damping cable system (CDCS), combining the advantages of damped cable for energy dissipation and double cables connected with cross ties for sag effect reduction. Not like dynamic vibration absorbers such as TMDs which may be effective only for one mode, dampers can suppress multi- mode vibration of the structure. The concept of double cables connected with cross ties was originally inspired by the researchers who proposed cross ties between cables in the cable-stayed bridges for suppressing wind-induced cable vibrations (Ahmad *et al*. 2018, Caracoglia and Jones 2007, Yamaguchi and Nagahawatta 1995, Zhou *et al*. 2015). In these studies, the damping effect of cross ties are utilized, while in our study double cables connected with cross ties are used to reduce the sag effect of the primary cable and thus improve the control performance of the primary damped cable. By introducing a restoring spring to ensure the primary cable always in the tension state, the energy dissipation of the damper connected with the primary cable is realized, and thus reduce the dynamic response of the structure. The authors have studied the control performance of CDCS for wind-Induced vibration control of high-rise structures when the cables are connected to structural column (Yu *et al*. 2021). In that study, the structure was treated as distributed parameter system, and taking the first vibration mode as the control object, an approximate solution of damping ratio was obtained. In this paper, the cable is connected to the lumped mass block on the top of the structure column, and the structure is treated as a lumped parameter model in theoretical derivation, and detailed parametric analysis is carried out to study the influence of various parameters on the control effect.

This paper first establishes the governing equations of the free vibration of the structure with CDCS system, and then solves the equation to obtain the analytical formula of the equivalent additional damping ratio. The accuracy of the analytical formula is verified by experimental model tests, and then influence factors of the equivalent additional damping ratio are analyzed. Finally forced vibration responses under harmonic and stochastic excitations are calculated to further verify the control performance of the CDCS.

2. System description and free vibration of structure with CDCS

It is known that the cable has sag effect, which leads to the reduction of axial tensile stiffness. According to Ernst's formula (Ernst 1965), the tensile equivalent elastic modulus of the cable as shown in Fig. 1(a) is obtained as

$$E_{eq} = \frac{E_e}{1 + \frac{\gamma^2 L^2}{12\sigma^3} E_e} = \mu E_e \tag{1}$$

where E_e is the elastic modulus of the cable material, γ is the gravity per unit volume of the cable, L is the span of the cable, and σ is the axial normal stress of the cable. For long-span cable, if σ remains the same, with the increase of span L, reduction factor of elastic modulus μ is approximately inverse proportional to quadratic cable span L^2.

In order to reduce the sag effect, we can increase the axial tensile stiffness by applying transverse forces perpendicular to the cable as shown in Fig. 1(b). With the

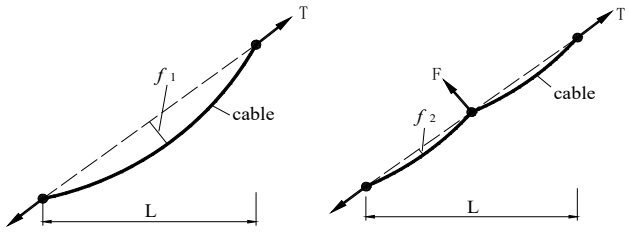

(a) Without transverse force (b) With transverse force

Fig. 1 Sag effect of stay cables

increase of the number of transverse external forces, the reduction factor of elastic modulus μ will gradually increase to close to one.

Based on the above principles, Sorace and Terenzi (2012a, b) proposed a single damped cable device. The device uses the guiding role of floor slab structure itself to exert transverse forces, but with the increase of structure height, the cable in the device tends to be parallel to the structure axis, and the damping performance will decrease rapidly. For high-rise structure with large height to width ratio, the single damped cable will lose its damping effect. At present, the high-rise structure mainly adopts TMDs to suppress wind-include vibration, which is difficult to suppress multi-mode and ultra-low frequency vibration of the structure. Inspired by the above principles and solving the limitations of the single damped cable device, Yu *et al.* invented a novel double cable damping device, i.e., compound damping cable system (Yu *et al.* 2014). Regardless of the height of the structure and the inclination of the CDCS, the value of μ for the main cable can always be guaranteed to be approximately equal to one, so that CDCS can be applied to the vibration suppressing of high-rise structures.

2.1 System components and vibration mitigation mechanism of CDCS

The schematic model of the CDCS for vibration reduction of high-rise structures is shown in Fig. 2. A structural column and a mass block are used to simulate the single mode vibration of high-rise structures. The CDCS is composed of a primary cable, a secondary cable, cross ties, a damper, restoring springs and other accessory components. The damper is in parallel with the restoring spring and they are connected in series with the primary cable. The pre-tension of the restoring spring ensures that the primary cable is always under tension. The secondary cable is in series with the spring, and the spring pre-tension also ensures that the secondary cable is in tension state. The primary cable is directly below the secondary cable and they are connected by the cross ties. Because the secondary cable has a large sag, it can bear all the gravity load of the primary cable and the secondary cable. Multiple cross ties are installed to provide transverse forces for the primary cable. The cross ties change the sag of the primary cable, and multiple cross ties with appropriate evenly distributed intervals along the primary cable can greatly reduce the sag of the primary cable, ensure the approximate linear state of the primary cable, and greatly improve the tensile stiffness of the primary cable.

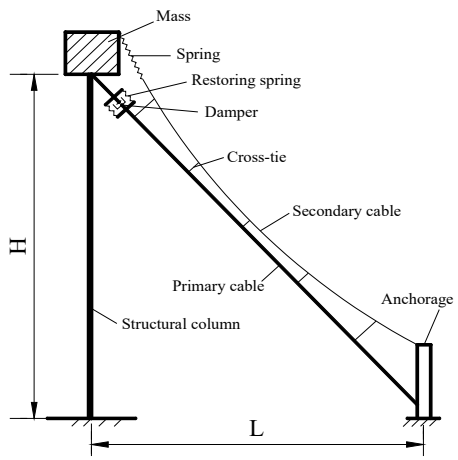

Fig. 2 The schematic model of the CDCS for vibration reduction of high-rise structures

When transverse vibration of the structure occurs, it results in larger relative displacement between the mass block and the ground anchor point. Since the tensile stiffness of the primary cable is much higher than that of the restoring spring, the deformation of the primary cable is very small and the two ends of the restoring spring has a relatively large displacement. By use of relative motion at the ends of the restoring spring to drive the energy dissipation damper, so as to reduce the vibration magnitude of the high- rise structure.

2.2 Governing equation for free vibration of structure with CDCS

With the method of modal analysis, the bending vibration of high-rise structures in arbitrary modes can be simplified into a single-degree-of-freedom (SDOF) model. In this study, only the first mode is considered since the structure is dominated by the first mode, and other modes can be also analysed in a similar way. Due to the tensile stiffness of the primary cable is far greater than that of the secondary cable, the tensile stiffness of the secondary cable and the mass of the main cable are ignored in this study. The high-rise structure with CDCS can be simplified into a two-degree-of-freedom system as shown in Fig. 3.

In this model, k_1 is the lateral stiffness of the structural column, k_2 is the stiffness of the restoring spring. k_3 is the tensile stiffness of the primary cable, c is the viscous damping coefficient of the damper, M is the lumped mass block at the top of the column, m is the mass of the restoring spring-damper device, and θ is the angle of inclination of the primary cable.

If not considering the structural inherent damping, the governing equation for free vibration of the structure with CDCS is

$$\begin{cases} M\cdot\ddot{x}_1 + c\dot{x}_1\cos^2\theta - c\dot{x}_2\cos\theta \\ +(k_1 + k_2\cos^2\theta)x_1 - k_2x_2\cos\theta = 0 \\ \\ m\ddot{x}_2 - c\dot{x}_1\cos\theta + c\dot{x}_2 - k_2x_1\cos\theta \\ +(k_2 + k_3)x_2 = 0 \end{cases} \tag{2}$$

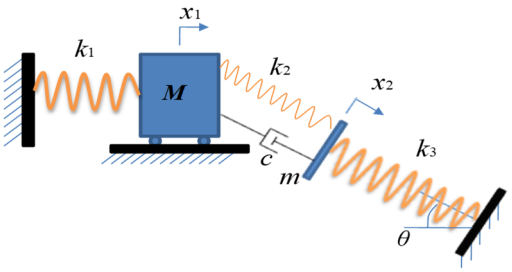

Fig. 3 Simplified model for high-rise structure with CDCS

where x_1 and x_2 are two independent coordinates. Since the mass of the restoring spring-damper device is very small and thus can be neglected, then Eq. (2) can be simplified as

$$cM \cdot \ddot{x}_1 + M(k_2 + k_3)\ddot{x}_1 + c(k_1 + k_3\cos^2\theta)\dot{x}_1 + (k_1k_2 + k_2k_3\cos^2\theta + k_1k_3)x_1 = 0 \quad (3)$$

where $\theta \neq 90^{\circ}$.

2.3 Closed form solution for additional damping ratio of structure with CDCS

In order to solve Eq. (3), assume the displacement of mass block as

$$x_1 = \chi e^{st} \quad (4)$$

where *s* is a constant to be determined. Substituting Eq. (4) into Eq. (3), it becomes

$$cMs^3 + M(k_2 + k_3)s^2 + c(k_1 + k_3\cos^2\theta)s + (k_1k_2 + k_2k_3\cos^2\theta + k_1k_3) = 0 \quad (5)$$

When the viscous damping coefficient of the damper $c = 0$, the undamped natural frequency of the system can be obtained

$$\omega_n = \sqrt{\frac{k_1k_2 + k_2k_3\cos^2\theta + k_1k_3}{(k_2 + k_3)M}} \quad (6)$$

When the viscous damping coefficient of the damper $c > 0$, set

$$\begin{cases} a_1 = cM \\ b_1 = M(k_2 + k_3) \\ c_1 = c(k_1 + k_3\cos^2\theta) \\ d_1 = (k_1k_2 + k_2k_3\cos^2\theta + k_1k_3) \end{cases} \quad (7)$$

Substituting Eq. (7) into Eq. (5), it becomes

$$a_1s^3 + b_1s^2 + c_1s + d_1 = 0 \quad (8)$$

Based on the root formulas of cubic equation (Shengjin's formulas) (Fan 1989), set

$$\begin{cases} A = b_1^2 - 3a_1c_1 \\ B = b_1c_1 - 9a_1d_1 \\ C = c_1^2 - 3b_1d_1 \end{cases} \quad (9)$$

The discriminant of multiple roots is $\Delta = B^2 - 4AC$. If $A = B = 0$, the equation has triple repeated real roots. If $\Delta > 0$, the equation has a real root and a pair of conjugate imaginary roots. If $\Delta = 0$, the equation has three real roots, two of which are double repeated roots. If $\Delta < 0$, the equation has three different real roots. For vibration reduction of high-rise structures, considering the balance of economic costs and structural safety, only small additional damping ratios is needed, therefore, the third order characteristic equation of the model will have virtual roots, and Δ must be greater than zero. If $\Delta > 0$, the three roots of the Eq. (8) are

$$s_1 = \frac{-b_1 - \left(\sqrt[3]{Y_1} + \sqrt[3]{Y_2}\right)}{3a_1} \quad (10)$$

$$s_2 = \frac{-b_1 + \frac{1}{2}\left(\sqrt[3]{Y_1} + \sqrt[3]{Y_2}\right) + \frac{\sqrt{3}}{2}\left(\sqrt[3]{Y_1} + \sqrt[3]{Y_2}\right)i}{3a_1} \quad (11)$$

$$s_3 = \frac{-b_1 + \frac{1}{2}\left(\sqrt[3]{Y_1} + \sqrt[3]{Y_2}\right) - \frac{\sqrt{3}}{2}\left(\sqrt[3]{Y_1} + \sqrt[3]{Y_2}\right)i}{3a_1} \quad (12)$$

where

$$Y_1 = Ab_1 + 3a_1\left(\frac{-B + \sqrt{B^2 - 4AC}}{2}\right),$$
$$Y_2 = Ab_1 + 3a_1\left(\frac{-B - \sqrt{B^2 - 4AC}}{2}\right)$$

and $i^2 = -1$.

Therefore, the general solution of the differential Eq. (3) is

$$x_1 = \chi_1 e^{s_1t} + e^{s_4t}(\chi_2 e^{is_5t} + \chi_3 e^{-is_5t}) \quad (13)$$

where

$$s_4 = \frac{-b_1 + \frac{1}{2}\left(\sqrt[3]{Y_1} + \sqrt[3]{Y_2}\right)}{3a_1}, \quad s_5 = \frac{\frac{\sqrt{3}}{2}\left(\sqrt[3]{Y_1} + \sqrt[3]{Y_2}\right)}{3a_1} \quad (14)$$

In Eq. (13), the first term is the real solution, the free vibration is only related to the complex solutions of the second and third terms, and the damping ratio of the system is

$$\xi = -\frac{s_4}{\omega_n} = -\frac{-b_1 + \frac{1}{2}\left(\sqrt[3]{Y_1} + \sqrt[3]{Y_2}\right)}{3a_1\omega_n} \quad (15)$$

3. Experimental validation

In order to verify the theoretical analysis results, a laboratory model test is carried out for the high-rise structure with CDCS. The relationship between the measured equivalent additional damping ratio of the structural model and various parameters is compared with the analytical solution of equivalent additional damping ratio derived in section 2.

3.1 Experimental model

The high-rise structure model is comprised of a rectangular steel column with a height of 3 m and a mass block of 160 kg installed at the top of the column. The rectangular hollow steel column has a section of 60 mm (length) × 40 mm (width) × 4 mm (thickness). The lower end of the column is anchored to the ground. This model can simulate the first order flexural motion of the high-rise structures. The compound damping cable system consists of a primary cable, a secondary cable, cross ties, an eddy current damper and a restoring spring. The primary cable, the secondary cable and the cross ties are all made from steel wire rope with diameters of 6.0 mm, 2.0 mm and 1.0 mm respectively. The eddy current damper and the restoring

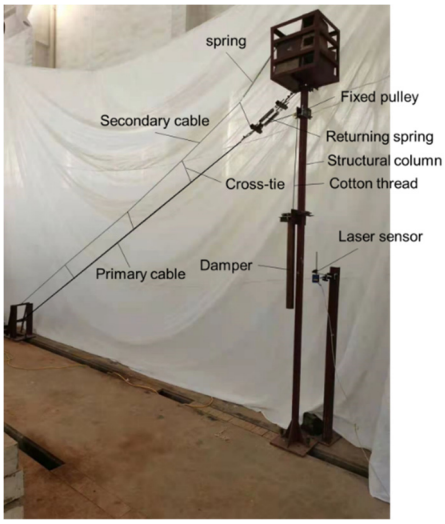

Fig. 4 Experiment site photos of high-rise structure and compound damping cable system

Table 1 Parameters of the experimental model

Parameter	Value	Parameter	Value
Height of column	3.0 m	Horizontal span of primary cable	5.0 m
Space between cross ties	1.5 m	Height of measurement point	1.55 m
Elastic modulus of primary cable	38 GPa	Elastic modulus of column	200 GPa
Mass of block mass	160 kg	Restoring spring stiffness for PC	3368 N/m
Diameter of primary cable	6 mm	Restoring spring stiffness for SC	395 N/m
Diameter of secondary cable	2 mm	Stiffness of the column	3956 N/m

spring are connected in series with the primary cable, and the eddy current damper is in parallel with the restoring spring. The noncontact laser displacement sensor is used to measure the vibration displacement of the structure to avoid increasing the additional damping ratio of the structure. The height of measurement point is 1.55 m. The eddy current damper is an ideal linear viscous damper when the relative velocity is low (Huang *et al*. 2018). The viscous damping coefficient is varied by changing the number of magnets in the experiments. The photo of model test is shown in Fig. 4. The parameters of the model are tabulated in Table 1.

3.2 Eddy-current damper

The structure of the eddy current damper is shown in Fig. 5. The eddy current damper is composed of copper tube, magnets and stainless steel rod. Neodymium-iron-boron magnets are installed on the stainless steel rod. The inner diameter of the copper tube is 55 mm, and the thickness of the copper tube is 5 mm. The outer diameter and the inner diameter of annular magnet blocks are 50 mm and 10 mm, respectively.

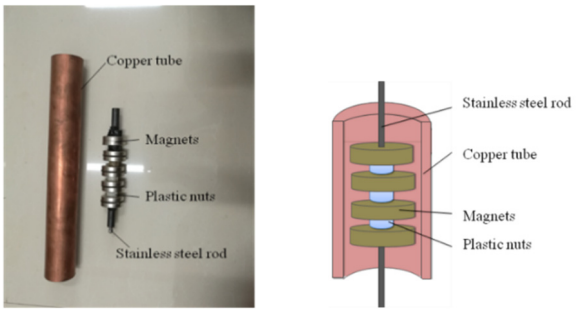

(a) Real photo (b) Schematic diagram

Fig. 5 Eddy current damper

Table 2 Viscous damping coefficients of eddy current dampers

Number of magnets	1	2	3	4	5
Viscous damping coefficient (Ns/m)	31	69	108	146	185

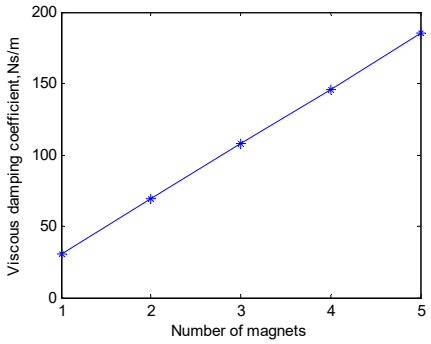

Fig. 6 Relationship between viscous damping coefficient of eddy current damper and number of magnets

In the test, plastic nuts with a thickness of 15 mm is installed between the magnets to isolate them. The thickness of magnets is 20 mm, and two adjacent magnets have the same pole. The viscous damping coefficients of eddy current dampers with different number of magnets are measured through experiments. The measured results are shown in Table 2 and Fig. 6.

3.3 Comparison of analytical and experimental results

Artificial excitations are used to make the structure vibrate. When the amplitude of the structure vibration reaches a set value, the excitation is suddenly removed and the structure continues to vibrate freely. The vibration displacement data are collected and the damping ratio is calculated by using the log decrement method (Feng *et al*. 2019). In order to eliminate the influence of amplitude on damping ratio estimation, the displacement data of attenuation section from amplitude 15 mm to 2 mm are selected to calculate damping ratio.

$$x = Ae^{-\xi\omega_n t}\sin(\omega_d t) \tag{16}$$

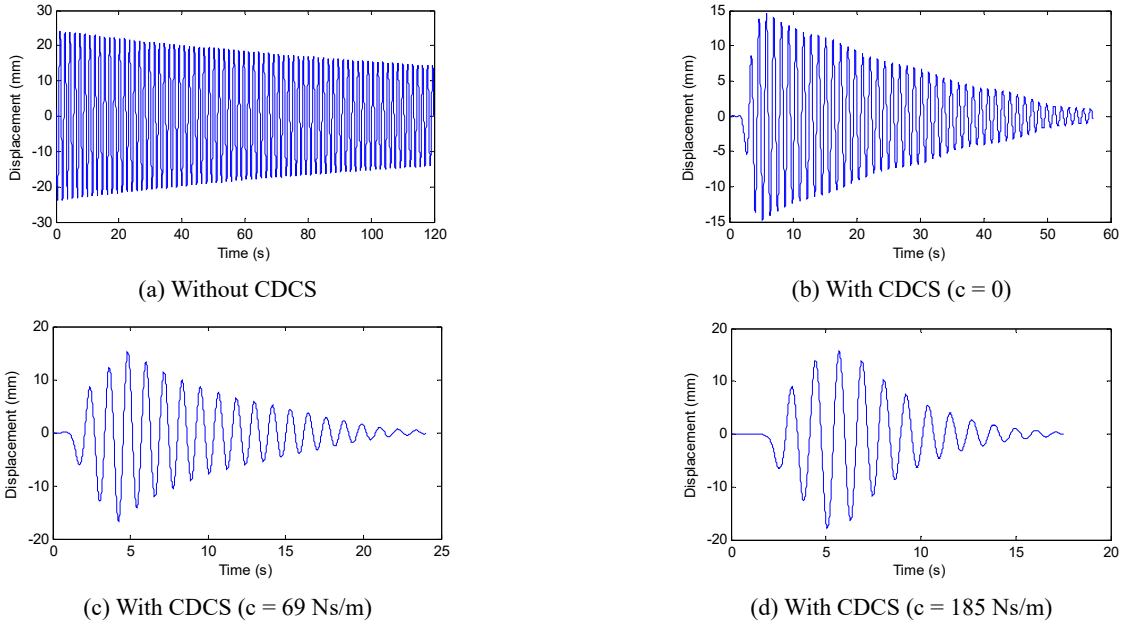

(a) Without CDCS (b) With CDCS (c = 0)

(c) With CDCS (c = 69 Ns/m) (d) With CDCS (c = 185 Ns/m)

Fig. 7 The displacement time histories of structure without and with CDCS

where, A is the initial amplitude of free vibration, ξ is the equivalent damping ratio, and ω_n is the natural frequency of the structure, $\omega_d = \omega_n\sqrt{1-\xi^2}$.

When the CDCS is not installed, the time history of structural vibration displacement is shown in Fig. 7(a), and the inherent damping ratio of the structure is 0.11%. After that, the CDCS is installed on the structure as shown in Fig. 3. The viscous damping coefficient is varied by changing the number of magnets in the eddy current damper. The measured displacement time histories of structural vibration with double-cable system but without damper is shown in Fig 7(b). The measured displacement time histories are shown in Figs. 7(c) and (d) respectively when the CDCS is installed with different damping coefficients of the eddy current damper. As can be seen from the figures, the CDCS can effectively dissipate the energy of structural vibration, making the vibration of the structure rapidly attenuate.

Eq. (15) is used to calculate theoretical values of equivalent additional damping ratio of the structure under various viscous damping coefficients of the ECD. The tested values of damping ratio are shown in Table 3. In order to eliminate the influence of amplitude on the calculation of damping ratio, the displacement data of the attenuation section from amplitude 15 mm to amplitude about 2 mm are uniformly selected to calculate the damping ratio. The comparison of the values of equivalent additional damping ratio of the structure under different viscous coefficients of the ECD is shown in Fig. 8.

According to Fig. 8 and Table 3, when the viscous damping coefficient of ECD increases from 0 Ns/m to 185 Ns/m, the measured equivalent damping ratio of the model structure increases from 0.55% to 5.41%. According to Eq. (15), the equivalent additional damping ratio of the structure increases from 0 to 4.56%. The measured values are slightly larger than the theoretical analysis results, and the trend of the two is consistent. The main reason for this difference is the existence of structural inherent damping (0.11%) and the friction of pulley in the model test, which leads to the test values slightly higher than the theoretical values.

Table 3 Experimental values of total damping ratio of the high-rise structure

c (Ns/m)	0	31	69	108	146	185
ζ (%)	0.55	1.23	2.38	3.31	3.95	5.41

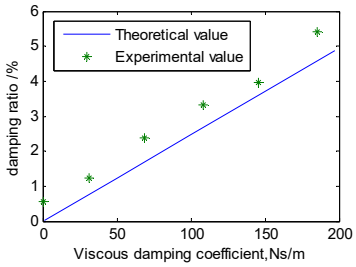

Fig. 8 Experimental values of total damping ratio and theoretical values of equivalent additional damping ratio

The measured results in Fig. 8 and Table 3 verify the theoretical analysis results of equivalent additional damping ratio of CDCS on high-rise structures. The influence of various parameters of CDCS on the damping effect of high-rise structure is further analyzed in the following section.

4. Parametric analysis

The parameters that affect the equivalent additional damping ratio of the structure include: flexural stiffness of the structural column, restoring spring stiffness, tensile stiffness of the primary cable, mass of the mass block,

damping coefficient of the damper, angle of inclination of the primary cable, etc. All the parameters are shown in Fig. 3 and Table 1. According to the analytic formula (15) of equivalent additional damping ratio provided by CDCS for high-rise structures, the influence rule of main parameters of CDCS on vibration reduction effect of high-rise structures is analyzed.

4.1 The influence of stiffness ratio

For the high-rise structure with CDCS, the total length of the primary cable and the restoring spring in series is always equal to the distance between the anchor point of the primary cable on the structure and the anchor point on the ground. When the ratio of the tensile stiffness of the primary cable to the stiffness of the restoring spring is larger, the deformation of the primary cable is smaller, and the deformation of the restoring spring is larger, leading to the larger deformation of the damper in parallel with the restoring spring, resulting in more energy dissipation, and better vibration reduction effect of the structure. For convenience of description, the stiffness ratio is defined as follows

$$\alpha_{ij} = \frac{k_i}{k_j} \qquad (i,j = 1,2,3) \tag{17}$$

where the meanings of k_i refer to Fig. 3. The effect of the stiffness ratio of the primary cable to the restoring spring is shown in Fig. 9, while the other parameters remain the same as shown in Table 1.

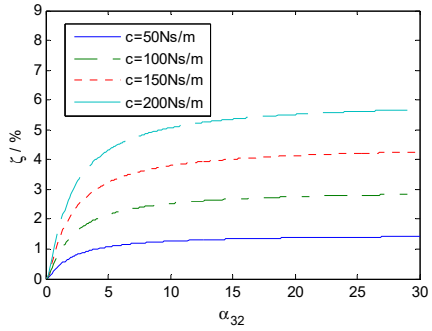

Fig. 9 Effect of stiffness ratio α_{32} on damping ratio

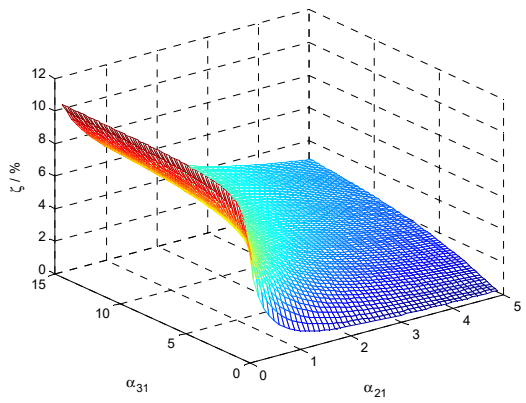

Fig. 10 Effects of stiffness ratio α_{31}, α_{21} on equivalent additional damping ratio

It can be seen from Fig. 9 that the equivalent additional damping ratio of the structure increases gradually with the gradual increase of stiffness ratio α_{32}, while it increases rapidly when the stiffness ratio is small and the increase speed decreases significantly when the stiffness ratio is larger than 5.

Change the stiffness of the primary cable and the stiffness of the restoring spring, keep the viscosity damping coefficient of the damper c = 180 Ns/m, and other parameters are shown in Table 1. The influence of the ratio of the primary cable stiffness to the flexural stiffness of the structure and the ratio of the restoring spring to the flexural stiffness of the structure on the equivalent additional damping ratio of the structure is shown in Fig. 10.

According to Fig. 10, increasing the stiffness ratio α_{31} can increase the equivalent additional damping ratio of the structure, while increasing the stiffness ratio α_{21} will reduce the equivalent additional damping ratio of the structure. According to the variation trend of damping ratio in Fig. 10, the relatively appropriate primary cable stiffness k_3 and restoring spring stiffness k_2 can be designed to provide an appropriate equivalent additional damping ratio for the structure and meet the vibration reduction requirements of high-rise structures.

4.2 The influence of angle of inclination of main cable

The primary cable inclination is another one of the important parameters affecting the vibration control performance of CDCS. Herein specify d = 6 mm and d = 2 mm for two kinds of primary cables, change the viscous damping coefficient of the damper and the angle of inclination of primary cable, the rest of the parameters remains the same as shown in Table 1. The relationship

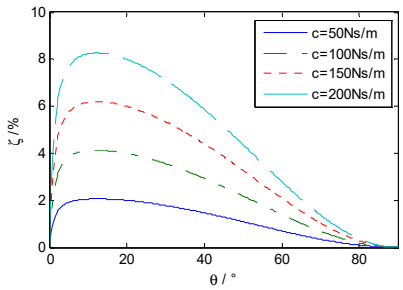

(a) d = 6 mm

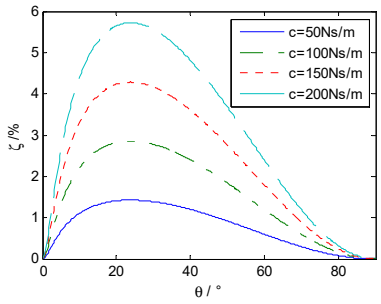

(b) d = 2 mm

Fig. 11 Effect of angle of inclination on equivalent additional damping ratio

between the equivalent additional damping ratio of the structure and the angle of inclination of the primary cable is calculated by Eq. (15), as shown in Figs. 11(a) and (b) respectively.

As can be seen from Fig. 11, when the angle of inclination of the primary cable increases, the equivalent additional damping ratio of the structure first increases and then decreases. For the primary cable with a diameter of d = 6 mm, the optimal angle of inclination θ_{opt} = 12.5° such that the CDCS can provide the maximum equivalent additional damping ratio for the structure. For the primary cable with a diameter of d = 2 mm, the optimal angle of inclination θ_{opt} = 23.8° such that the CDCS can provide the maximum equivalent additional damping ratio for the structure. As the diameter of primary cable increases, its optimal inclination angle of inclination decreases. The larger the diameter of the primary cable, the larger the additional damping ratio of the damped cable can provide for the structure.

It can be seen from Figs. 8, 9 and 11 that in the case of small damping, increasing the damping coefficient of the ECD can increase the equivalent additional damping ratio of the structure, which is proportional to the viscous damping coefficient of the damper.

5. Forced vibration of structure with CDCS

5.1 The response to harmonic excitation

Assume the mass block to be subjected to harmonic excitation, and the structural vibration equation is

$$\begin{cases} M\cdot\ddot{x}_1 + c\dot{x}_1\cos^2\theta - c\dot{x}_2\cos\theta + (k_1 + k_2\cos^2\theta)x_1 \\ -k_2x_2\cos\theta = F_0\sin(\Omega t) \\ m\ddot{x}_2 - c\dot{x}_1\cos\theta = F_0\sin(\Omega t) \end{cases} \tag{18}$$

Since the mass of the restoring spring-damper device is very small and thus can be neglected, then Eq. (18) can be simplified as

$$\begin{aligned} &cM\cdot\ddot{x}_1 + M(k_2+k_3)\ddot{x}_1 + c(k_1 + k_3\cos^2\theta)\dot{x}_1 \\ &+(k_1k_2 + k_2k_3\cos^2\theta + k_1k_3)x_1 \\ &= (k_2+k_3)F_0\sin(\Omega t) + c\Omega F_0\sin(\Omega t) \end{aligned} \tag{19}$$

Set the vibration displacement of mass block as

$$x_1 = X_s\sin(\Omega t - \phi_s) + X_c\cos(\Omega t - \phi_c) \tag{20}$$

Substitute Eq. (20) into Eq. (19) and get

$$X_s = \frac{(k_2+k_3)F_0}{\sqrt{(c_1\Omega - a_1\Omega^3)^2 + (d_1 - b_1\Omega^2)^2}} \tag{21}$$

$$X_c = \frac{c\Omega F_0}{\sqrt{(c_1\Omega - a_1\Omega^3)^2 + (d_1 - b_1\Omega^2)^2}} \tag{22}$$

$$\tan(\phi_s) = \tan(\phi_c) = \frac{c_1\Omega - a_1\Omega^3}{d_1 - b_1\Omega^2} \tag{23}$$

where, a_1, b_1, c_1 and d_1 are shown in Eq. (7), and Eq. (20) is rewritten as

$$x_1 = X\sin(\Omega t - \phi_s + \phi) = X\cos(\Omega t - \alpha) \tag{24}$$

where

$$X = \sqrt{X_S^2 + X_C^2} \tag{25}$$

$$\tan(\varphi) = \frac{X_c}{X_s} \tag{26}$$

The structural static deformation ($\Omega = 0$) can be obtained as

$$X_0 = \frac{(k_2+k_3)F_0}{k_1k_2 + k_2k_3\cos^2\theta + k_1k_3} \tag{27}$$

Dynamic amplification coefficient is defined as $D_s = X/X_0$, and the frequency ratio is $r = \Omega/\omega_n$. The amplitude-frequency characteristics of the tested model are shown in Fig. 12, and phase-frequency characteristics are shown in Fig. 13.

As can be seen from Fig. 12, when the external excitation frequency is close to the natural frequency of the structure, the structure resonates with large vibration amplitude. With the increase of the viscosity damping coefficient of the damper, the vibration amplitude of the structure significantly decreases. As shown in Fig. 13, the phase angle increases with the increase of frequency ratio, and the increase speed will decrease with the increase of viscosity damping coefficient of the damper, which indicates damping will slow down the changes of the phase angle.

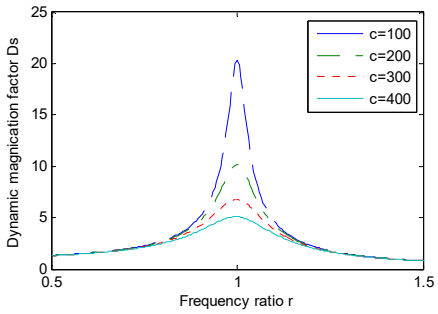

Fig. 12 Variation of dynamic magnification factor with damping and frequency

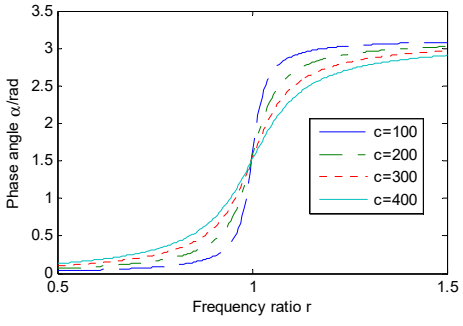

Fig. 13 Variation of phase angle with damping and frequency

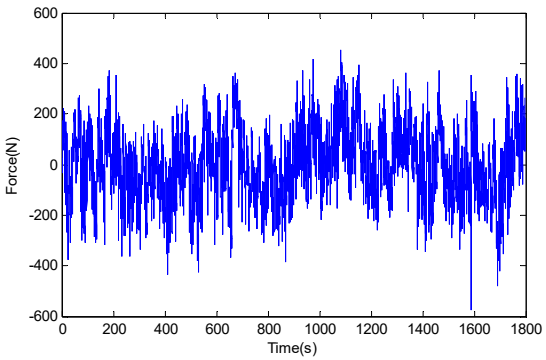

Fig. 14 Time history of wind load

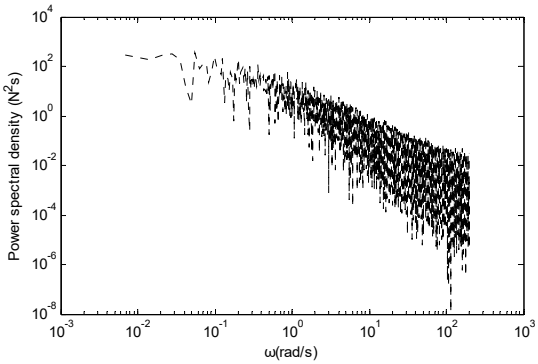

Fig. 15 PSD of wind load

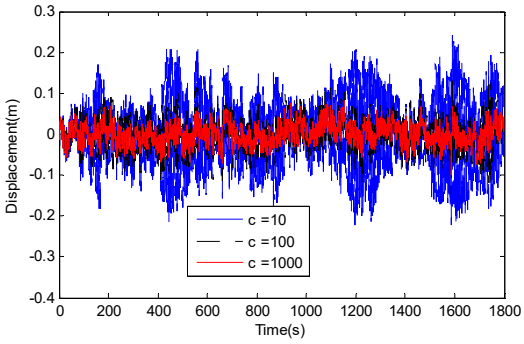

(a) 30 minute period

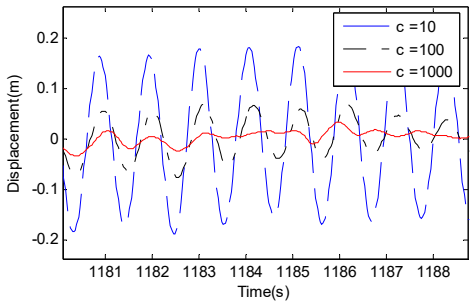

(b) Short time period

Fig. 16 The time history of structural displacement response under the action of fluctuating wind

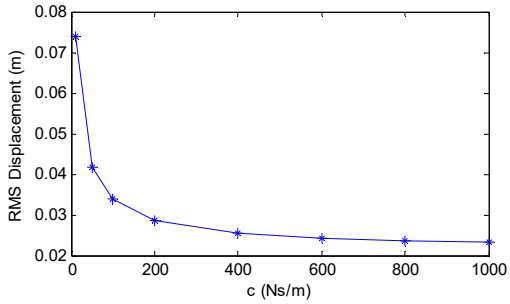

Fig. 17 The relationship between the root-mean-square of structural displacement response and the viscous damping coefficient of the damper

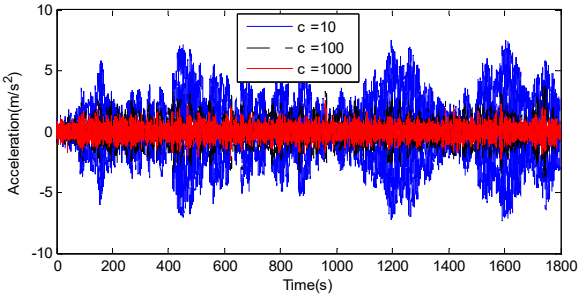

(a) 30 minute period

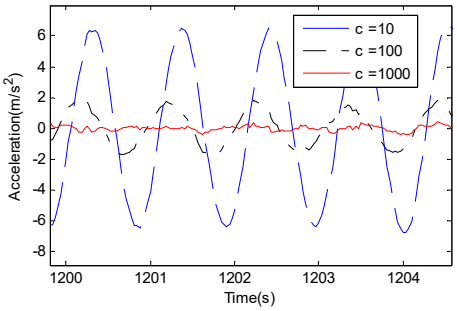

(b) Short time period

Fig. 18 The time history of structural acceleration response under the action of fluctuating wind

5.2 The response to stochastic excitation

In this section, a set of field measured fluctuating wind speed data are utilized to simulate stochastic wind loads applied on the structure. By converting wind speed to wind loading, the time history of the wind load is shown in Fig. 14 and its power spectral density is shown in Fig. 15. The angle of inclination for the primary damped cable $\theta = 45°$, The remaining parameters are shown in Table 1.

Step-by-step integration approach is adopted to calculate the structural vibration responses subjected to fluctuating wind. The time histories of displacement response with different viscous damping coefficients of the damper are shown in Fig. 16. When the viscous damping coefficient of the damper is small, the structure resonates, along with the

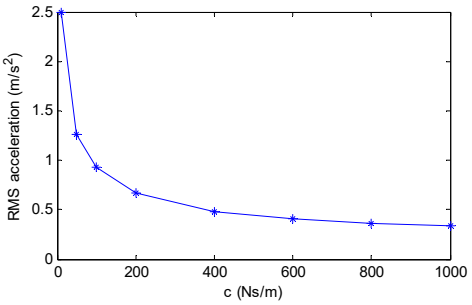

Fig. 19 The relationship between root-mean-square of acceleration and viscous damping coefficient of the damper

rising of viscous damping coefficient, vibration amplitude decreases. The relationship between the root-mean-square of structural displacement and the viscous damping coefficient of the damper is shown in Fig. 17.

The time histories of acceleration response with different viscous damping coefficients of the damper are shown in Fig. 18. When the viscous damping coefficient is small, the structure shows resonance phenomenon and the vibration acceleration is large. With the increase of viscous damping coefficient, the vibration acceleration decreases. The relationship between root-mean-square of acceleration and viscous damping coefficient of the damper is shown in Fig. 19.

6. Conclusions

This paper introduces a novel compound damping cable system for vibration reduction of high-rise structures. The governing equations for free vibration are established first and then solved according to Shengjin's formulas, as a result, the explicit analytic solution of equivalent additional damping ratio of the structure is obtained. The accuracy of the analytic solution is verified by laboratory model test, and the influence of several main parameters in the system on the equivalent additional damping ratio of the structure is analyzed, and finally the forced vibration responses under harmonic and stochastic wind loads are calculated to further verify the effect of the vibration control performance. Based on the analysis, the following conclusions are drawn:

- The analytical formula of the equivalent additional damping ratio can accurately model the damping effect of the CDCS, and the CDCS can provide a large equivalent additional damping ratio for high-rise structures.
- The equivalent additional damping ratio of the structure increases with the increase of the viscous damping coefficient of the damper, and the relationship of the two are approximately proportional.
- Increasing the stiffness of the primary cable is conducive to improving its damping effect on the structure. When the stiffness ratio of the primary cable to the restoring spring is less than 5, the equivalent additional damping ratio of the structure increases rapidly with the increase of the stiffness ratio, but it increases much slowly when the stiffness ratio is larger than 5. However, if the stiffness ratio of the restoring spring to the bending stiffness of the structure increases, the equivalent additional damping ratio of the structure will decrease. Therefore, the stiffness of the restoring spring should be reduced as much as possible.
- When the angle of inclination for the damped cable increases from 0° to 90°, the equivalent additional damping ratio increases rapidly at first, reaches the maximum value, and then decreases gradually. The optimal angle of inclination for the damped cable can be obtained at the maximum equivalent additional damping ratio of the CDCS to the high-rise structure.
- Under the action of simple harmonic excitation, when the excitation frequency is close to the natural frequency of the structure, the structure will vibrate greatly. With the increase of the viscous damping coefficient of the damper in the CDCS, the resonance amplitude of the structure will decrease rapidly.
- Under the action of stochastic load, when the viscous damping coefficient of the damper is small, the structure exhibits approximate harmonic vibration with large amplitude. With the increase of the viscous damping coefficient of the damper, the amplitudes of the displacement and the acceleration of the structure decrease significantly, showing random vibration.

Acknowledgments

This research was supported in part by Key Project of Scientific Research Fund (grant No.17A071) from Education Department of Hunan Province, the independent research project fund from the State Key Laboratory of Advanced Design and Manufacturing for Vehicle Body in Hunan University (grant No. 71865006) and the Fundamental Research Funds for the Central Universities (grant No. 531118010047).

References

Ahmad, J., Cheng, S. and Ghrib, F. (2018), "Combined effect of external damper and crosstie on the modal response of hybrid two-cable networks", *J. Sound Vib.*, **417**, 132-148. https://doi.org/10.1016/j.jsv.2017.12.023

Aly, A.M., Zasso, A. and Resta, F. (2011), "On the dynamics of a very slender building under winds: response reduction using M R dampers with lever mechanism", *Struct. Des. Tall Special Build.*, **20**(5), 539-551. https://doi.org/10.1002/tal.647

Benavent-Climent, A. (2011), "An energy based method for seismic retrofit of existing frames using hysteretic dampers", *Soil Dyn. Earthq. Eng.*, **31**(10), 1385-1396. https://doi.org/10.1016/j.soildyn.2011.05.015

Caracoglia, L. and Jones, N.P. (2007), "Passive hybrid technique for the vibration mitigation of systems of interconnected stays", *J. Sound Vib.*, **307**(3-5), 849-864. https://doi.org/10.1016/j.jsv.2007.07.022

Chen, Z.Q., Wang, X.Y., Ko, J.M., Ni, Y.Q., Spencer Jr, B.F., Yang, G. and Hu, J.H. (2004), "MR damping system for mitigating wind-rain induced vibration on Dongting Lake Cable-Stayed Bridge", *Wind Struct*., *Int*. *J*., **7**(5), 293-304. https://doi.org/10.12989/was.2004.7.5.293

Choi, S.-W. and Kim, H.-K. (2008), "Design of aerodynamic stabilizing cables for a cable-stayed bridge during construction", *Wind Struct*., *Int*. *J*., **11**(5), 391-411. https://doi.org/10.12989/was.2008.11.5.391

Duan, Y., Ni, Y.-Q., Zhang, H., Spencer, B.F.J., Ko, J.-M. and Fang, Y. (2019), "Design formulas for vibration control of taut cables using passive MR dampers", *Smart Struct*. *Syst*., *Int*. *J*., **23**(6), 521-536. https://doi.org/10.12989/sss.2019.23.6.521

Ernst, J.H. (1965), "Der E-modul von seilen under berücksichtigung des durchhanges", *Bauing*, **40**(2), 52-55.

Fan, S. (1989), "A new extracting formula and a new distinguishing means on the one variable cubic equation", *J*. *Hainan Normal Univ*. (*Nat*. *Sci*.), **2**(2), 91-98.

Feng, Z.Q., Zhao, B., Hua, X.G. and Chen, Z.Q. (2019), "Enhanced EMD-RDT Method for Output-Only Ambient Modal Identification of Structures", *J*. *Aerosp*. *Eng*., **32**(4), 04019046. https://doi.org/10.1061/(ASCE)AS.1943-5525.0001034

Gao, H., Wang, H., Li, J., Wang, Z., Liang, R., Xu, Z. and Ni, Y. (2021), "Optimum design of viscous inerter damper targeting multi-mode vibration mitigation of stay cables", *Eng*. *Struct*., **226**, 111375. https://doi.org/10.1016/j.engstruct.2020.111375

Huang, Z.W., Hua, X.G., Chen, Z.Q. and Niu, H.W. (2018), "Modeling, Testing, and Validation of an Eddy Current Damper for Structural Vibration Control", *J*. *Aerosp*. *Eng*., **31**(5), 04018063. https://doi.org/10.1061/(ASCE)AS.1943-5525.0000891

Huang, Z., Hua, X., Chen, Z. and Niu, H. (2019), "Performance evaluation of inerter-based damping devices for structural vibration control of stay cables", *Smart Struct*. *Syst*., *Int*. *J*., **23**(6), 615-626. https://doi.org/10.12989/sss.2019.23.6.615

Ikago, K., Saito, K. and Inoue, N. (2012a), "Seismic control of single-degree-of-freedom structure using tuned viscous mass damper", *Earthq*. *Eng*. *Struct*. *Dyn*., **41**(3), 453-474. https://doi.org/10.1002/eqe.1138

Ikago, K., Sugimura, Y., Saito, K. and Inoue, N. (2012b), "Modal Response Characteristics of a Multiple-Degree-Of-Freedom Structure Incorporated with Tuned Viscous Mass Dampers", *J*. *Asian Architect*. *Build*. *Eng*., **11**(2), 375-382. https://doi.org/10.3130/jaabe.11.375

Kim, H.-K., Kim, K.-T., Lee, H. and Kim, S. (2013), "Performance of Unpretensioned Wind Stabilizing Cables in the Construction of a Cable-Stayed Bridge", *J*. *Bridge Eng*., **18**(8), 722-734. https://doi.org/10.1061/(ASCE)BE.1943-5592.0000405

Lazar, L.F., Neild, S.A. and Wagg, D.J. (2014), "Using an inerter-based device for structural vibration suppression", *Earthq*. *Eng*. *Struct*. *Dyn*., **43**(8), 1129-1147. https://doi.org/10.1002/eqe.2390

Li, H., Liu, M., Li, J., Guan, X. and Ou, J. (2007), "Vibration Control of Stay Cables of the Shandong Binzhou Yellow River Highway Bridge Using Magnetorheological Fluid Dampers", *J*. *Bridge Eng*., **12**(4), 401-409. https://doi.org/10.1061/(ASCE)1084-0702(2007)12:4(401)

Li, L., Song, G. and Ou, J. (2011), "Hybrid active mass damper (AMD) vibration suppression of nonlinear high-rise structure us-ing fuzzy logic control algorithm under earthquake excitations", *Struct*. *Control Health Monitor*., **18**(6), 698-709. https://doi.org/10.1002/stc.402

Liang, L., Feng, Z. and Chen, Z. (2019), "Seismic control of SDOF systems with nonlinear eddy current dampers", *Appl*. *Sci*., **9**(16), 3427. https://doi.org/10.3390/app9163427

Lin, W.-H. and Chopra, A.K. (2002), "Earthquake response of elastic SDF systems with non-linear fluid viscous dampers", *Earthq*. *Eng*. *Struct*. *Dyn*., **31**(9), 1623-1642. https://doi.org/10.1002/eqe.179

Lin, W., Song, G. and Chen, S. (2017), "PTMD Control on a Benchmark TV Tower under Earthquake and Wind Load Excitations", *Appl*. *Sci*.*-Basel*, **7**(4), 425. https://doi.org/10.3390/app7040425

Liu, W., Guo, Y., Dong, X. and He, W. (2019), "Earthquake response control of a super high-rise structure subjected to long-period ground motions via a novel viscous damped system with multilever mechanism", *Struct*. *Des*. *Tall Special Build*., **28**(7), e1600. https://doi.org/10.1002/tal.1600

Lu, X., Zhang, Q., Weng, D., Zhou, Z., Wang, S., Mahin, S.A., Ding, S. and Qian, F. (2017), "Improving performance of a super tall building using a new eddy-current tuned mass damper", *Struct*. *Control Health Monitor*., **24**(3), e1882. https://doi.org/10.1002/stc.1882

Mao, J.-X., Wang, H., Feng, D.-M., Tao, T.-Y. and Zheng, W.-Z. (2018), "Investigation of dynamic properties of long-span cable stayed bridges based on one-year monitoring data under normal operating condition", *Struct*. *Control Health Monitor*., **25**(5), e2146. https://doi.org/10.1002/stc.2146

Ni, Y.Q., Wang, J.Y. and Lo, L.C. (2005), "Influence of Stabilizing Cables on Seismic Response of a Multispan Cable Stayed Bridge", *Comput*.*-Aided Civil Infrastruct*. *Eng*., **20**(2), 142-153. https://doi.org/10.1111/j.1467-8667.2005.00383.x

Niu, H., Chen, Z., Hua, X. and Zhang, W. (2018), "Mitigation of wind-induced vibrations of bridge hangers using tuned mass dampers with eddy current damping", *Smart Struct*. *Syst*., *Int*. *J*., **22**(6), 727-741. https://doi.org/10.12989/sss.2018.22.6.727

Pan, C. and Zhang, R. (2018), "Design of structure with inerter system based on stochastic response mitigation ratio", *Struct*. *Control Health Monitor*., **25**(6), e2169. https://doi.org/10.1002/stc.2169

Pan, C., Zhang, R., Luo, H., Li, C. and Shen, H. (2018), "Demand-based optimal design of oscillator with parallel-layout viscous in-erter damper", *Struct*. *Control Health Monitor*., **25**(1), e2051. https://doi.org/10.1002/stc.2051

Roy, S., Park, Y.C., Sause, R. and Fisher, J.W. (2012), "Fatigue Performance of Stiffened Pole-to-Base Plate Socket Connections in High-Mast Structures", *J*. *Struct*. *Eng*., **138**(10), 1203-1213. https://doi.org/10.1061/(ASCE)ST.1943-541X.0000554

Shen, W., Niyitangamahoro, A., Feng, Z. and Zhu, H. (2019), "Tuned inerter dampers for civil structures subjected to earthquake ground motions: optimum design and seismic performance", *Eng*. *Struct*., **198**, 109470. https://doi.org/10.1016/j.engstruct.2019.109470

Shi, X., Zhu, S., Li, J.-Y. and Spencer Jr., B.F. (2016), "Dynamic behavior of stay cables with passive negative stiffness dampers", *Smart Mater*. *Struct*., **25**(7), 075044. https://doi.org/10.1088/0964-1726/25/7/075044

Sorace, S. and Terenzi, G. (2012a), "The damped cable system for seismic protection of frame structures - Part I: General concepts, testing and modeling", *Earthq*. *Eng*. *Struct*. *Dyn*., **41**(5), 915-928. https://doi.org/10.1002/eqe.1166

Sorace, S. and Terenzi, G. (2012b), "The damped cable system for seismic protection of frame structures - Part II: Design and appli-cation", *Earthq*. *Eng*. *Struct*. *Dyn*., **41**(5), 929-947. https://doi.org/10.1002/eqe.1165

Suarez, E., Roldán, A., Gallego, A. and Benavent-Climent, A. (2017), "Entropy analysis for damage quantification of hysteretic dampers used as seismic protection of buildings", *Appl*. *Sci*., **7**(6), 628. https://doi.org/10.3390/app7060628

Sun, C., Jahangiri, V. and Sun, H. (2019a), "Performance of a 3D pendulum tuned mass damper in offshore wind turbines under multiple hazards and system variations", *Smart Struct*. *Syst*., *Int*. *J*., **24**(1), 53-65. https://doi.org/10.12989/sss.2019.24.1.053

Sun, H., Zuo, L., Wang, X., Peng, J. and Wang, W. (2019b), "Exact H 2 optimal solutions to inerter-based isolation systems for building structures", *Struct. Control Health Monitor.*, **26**(6), e2357. https://doi.org/10.1002/stc.2357

Wang, Z., Gao, H., Xu, Y., Chen, Z. and Wang, H. (2019a), "Impact of cable sag on the efficiency of an inertial mass damper in controlling stay cable vibrations", *Smart Struct. Syst., Int. J.*, **24**(1), 83-94. https://doi.org/10.12989/sss.2019.24.1.083

Wang, Z.H., Xu, Y.W., Gao, H., Chen, Z.Q., Xu, K. and Zhao, S.B. (2019b), "Vibration control of a stay cable with a rotary electromagnetic inertial mass damper", *Smart Struct. Syst., Int. J.*, **23**(6), 627-639. https://doi.org/10.12989/sss.2019.23.6.627

Wen, Y., Chen, Z. and Hua, X. (2017), "Design and Evaluation of Tuned Inerter-Based Dampers for the Seismic Control of MDOF Structures", *J. Struct. Eng.*, **143**(4), 04016207. https://doi.org/10.1061/(ASCE)ST.1943-541X.0001680

Yamaguchi, H. and Nagahawatta, H.D. (1995), "Damping effects of cable cross ties in cable-stayed bridges", *J. Wind Eng. Indust. Aerodyn.*, **54-55**, 35-43. https://doi.org/10.1016/0167-6105(94)00027-B

Yu, J., Tang, Y., Zhu, Y., Yu, P. and Wang, X. (2014), "A compound damping cable system", Chinese Invention Patent, CN104404886B.

Yu, J., Duan, Z., Zhang, X., Peng, J., Zhao, Y. (2021), "Wind-Induced Vibration Control of High-Rise Structures Using Compound Damping Cables", *Shock Vib.*, **2021**, 5537622. https://doi.org/10.1155/2021/5537622

Zahrai, S.M. and Froozanfar, M. (2019), "Performance of passive and active MTMDs in seismic response of Ahvaz cable-stayed bridge", *Smart Struct. Syst., Int. J.*, **23**(5), 449-466. https://doi.org/10.12989/sss.2019.23.5.449

Zhang, P., Song, G., Li, H.-N. and Lin, Y.-X. (2013), "Seismic Control of Power Transmission Tower Using Pounding TMD", *J. Eng. Mech.*, **139**(10), 1395-1406. https://doi.org/10.1061/(ASCE)EM.1943-7889.0000576

Zhang, Z., Nielsen, S.R.K., Basu, B. and Li, J. (2015), "Nonlinear modeling of tuned liquid dampers (TLDs) in rotating wind turbine blades for damping edgewise vibrations", *J. Fluids Struct.*, **59**, 252-269. https://doi.org/10.1016/j.jfluidstructs.2015.09.006

Zhang, Z., Staino, A., Basu, B. and Nielsen, S.R.K. (2016), "Performance evaluation of full-scale tuned liquid dampers (TLDs) for vibration control of large wind turbines using real time hybrid testing", *Eng. Struct.*, **126**, 417-431. https://doi.org/10.1016/j.engstruct.2016.07.008

Zhang, R., Ni, Y.-Q., Duan, Y. and Ko, J.-M. (2019a), "Development of a full-scale magnetorheological damper model for open-loop cable vibration control", *Smart Struct. Syst., Int. J.*, **23**(6), 553-564. https://doi.org/10.12989/sss.2019.23.6.553

Zhang, R., Zhao, Z. and Dai, K. (2019b), "Seismic response mitigation of a wind turbine tower using a tuned parallel inerter mass system", *Eng. Struct.*, **180**, 29-39. https://doi.org/10.1016/j.engstruct.2018.11.020

Zhou, H., Yang, X., Sun, L. and Xing, F. (2015), "Free vibrations of a two-cable network with near-support dampers and a cross-link", *Struct. Control Health Monitor.*, **22**(9), 1173-1192. https://doi.org/10.1002/stc.1738

Zuo, L., Chen, X. and Nayfeh, S. (2011), "Design and Analysis of a New Type of Electromagnetic Damper with Increased Energy Density", *J. Vib. Acoust.*, **133**(4), 041006. https://doi.org/10.1115/1.4003407.

Zuo, H., Bi, K. and Hao, H. (2017), "Using multiple tuned mass dampers to control offshore wind turbine vibrations under multi-ple hazards", *Eng. Struct.*, **141**, 303-315. https://doi.org/10.1016/j.engstruct.2017.03.006